

Defect induced room-temperature ferromagnetism and enhanced photocatalytic activity in Ni-doped ZnO synthesized by electrodeposition

Deepika, Raju Kumar, Ritesh Kumar, Kamdeo Prasad Yadav, Pratyush Vaibhav, Seema Sharma, Rakesh Kumar Singh, Santosh Kumar

Citation: Chin. Phys. B . 2020, 29(10): 108503 . **doi:** 10.1088/1674-1056/ab9c0c
Journal homepage: http://cpb.iphy.ac.cn; http://iopscience.iop.org/cpb

What follows is a list of articles you may be interested in

Homogeneous and inhomogeneous magnetic oxide semiconductors

Xiao-Li Li(李小丽), Xiao-Hong Xu(许小红)

Chin. Phys. B . 2019, 28(9): 098506 . **doi:** 10.1088/1674-1056/ab38ac

Enhanced light emission from InGaN/GaN quantum wells by using surface plasmonic resonances of silver nanoparticle array

Chen Zhan-Xu, Wan Wei, Zhang Bai-Jun, He Ying-Ji, Jin Chong-Jun

Chin. Phys. B . 2014, 23(12): 128504 . **doi:** 10.1088/1674-1056/23/12/128504

A novel strong green phosphor：$K_3Gd(PO_4)_2$：Ce^{3+}, Tb^{3+} for a UV-excited white light-emitting-diode

Jiang Ting-Ming, Yu Xue, Xu Xu-Hui, Zhou Da-Cheng, Yu Hong-Ling, Yang Peng-Hui, Qiu Jian-Bei

Chin. Phys. B . 2014, 23(2): 028505 . **doi:** 10.1088/1674-1056/23/2/028505

Characterization and luminescence of Eu/Sm-coactivated $CaYAl_3O_7$ phosphor synthesized by using a combustion method

Yu Hong-Ling, Yu Xue, Xu Xu-Hui, Jiang Ting-Ming, Yang Peng-Hui, Jiao Qing, Zhou Da-Cheng, Qiu Jian-Bei

Chin. Phys. B . 2013, 22(9): 098503 . **doi:** 10.1088/1674-1056/22/9/098503

Oxide magnetic semiconductors：Materials, properties, and devices

Tian Yu-Feng, Hu Shu-Jun, Yan Shi-Shen, Mei Liang-Mo

Chin. Phys. B . 2013, 22(8): 088505 . **doi:** 10.1088/1674-1056/22/8/088505

Defect induced room-temperature ferromagnetism and enhanced photocatalytic activity in Ni-doped ZnO synthesized by electrodeposition*

Deepika[1], Raju Kumar[1], Ritesh Kumar[1], Kamdeo Prasad Yadav[1], Pratyush Vaibhav[2], Seema Sharma[3], Rakesh Kumar Singh[4], and Santosh Kumar[1,†]

[1] College of Commerce, Arts and Science, Patna, Bihar, India
[2] Jaypee University of Engineering and Technology, Guna, Madhya Pradesh, India
[3] Anugrah Narayan College, Patna, Bihar, India
[4] Aryabhatta Knowledge University, Patna, Bihar, India

(Received 16 April 2020; revised manuscript received 16 May 2020; accepted manuscript online 12 June 2020)

$Zn_{0.90}Ni_{0.10}O$ nanoparticles have been synthesized by single-bath two-electrode electrodeposition at constant voltage. X-ray diffraction, UV vis and photoluminescence studies reveal that a single-phase polycrystalline hcp wurtzite crystal structure of ZnO is evolved. The material consists of a large number of defects such as oxygen vacancy (O_v) and zinc interstitial (Zi). The magnetization study reveals that the sample exhibits room-temperature global ferromagnetism and the ferromagnetic ordering seems to be defect induced via bound magnetic polaron mechanism, and double exchange is also expected to have played role. Interesting optoelectronic properties have been found in the synthesized sample and the material seems to be a potential candidate to be used as a UV sensor. Such a transition metal doped ZnO based dilute magnetic semiconducting system exhibiting room-temperature ferromagnetism is likely to be first of its kind in the sense that such materials have not yet been reported to be synthesized by the simple method of electrodeposition to the best of our knowledge on the basis of ample literature review.

Keywords: dilute magnetic semiconductors (DMS), bound magnetic polaron, photoluminescence, ferromagnetism

PACS: 85.75.–d, 75.25.–j, 75.30.Cr, 75.30.Et **DOI:** 10.1088/1674-1056/ab9c0c

1. Introduction

Manipulating physical properties of a material by introducing a dopant in the matrix of a solid semiconducting host to realize a desired functionality has attracted a great deal of attention since the last few decades. Magnetic and optoelectronic properties have been tailored by controlled doping in semiconductors to obtain interesting useful functionalities. Significant researches are being performed to explore the possibilities of inducing ferromagnetism (FM) by controlling spin degree of freedom of electrons in otherwise nonmagnetic semiconductors by doping dilute concentrations of magnetic impurities therein.[1–5] This field of research is categorized as the field of dilute magnetic semiconductors (DMS).[6–19] Dilute Doping ensures that besides the original application specific non-magnetic set of properties of the undoped parent material remain widely unaffected, an FM can also be induced in the material enabling us the best uses of both the properties.[20]

Magnetic properties of Ni-doped ZnO thin films have been studied by Wakano *et al.*[21] They have reported that the solubility of Ni in ZnO is up to 25% without precipitation. Ferromagnetism was observed at 2 K for the film doped with 3–35% of Ni. Above 30 K, superparamagnetic behavior has been observed. Schwartz *et al.*[22] have observed robust ferromagnetism with T_c of about 350 K in Ni-doped ZnO nano crystalline thin films prepared using high quality colloidal DMS quantum dots as solution precursors. Apart from ferromagnetism, a substantial superparamagnetism was also observed in zero-field-cooled and field-cooled magnetization studies.

Radonovic *et al.*[23] have reported ferromagnetism in Ni-doped ZnO DMS systems synthesized from solution with $T_c >$ 350 K. Colloidal Ni^{2+}: ZnO nano crystals have been reported to be paramagnetic but their aggregation has been found to be exhibiting ferromagnetism, which may be attributed to the increase in domain volumes and the generation of new lattice defects during aggregation.

Room-temperature ferromagnetism (RTFM) with low moment in Ni-doped ZnO nanoparticles (NPs) has been reported by Srinet *et al.*, in which the material synthesis was carried out by a sol-gel route.[24] RTFM has also been reported by Liu *et al.* in Ni-doped ZnO films synthesized by pulsed laser deposition.[25] RTFM is reported in ZnO films for Ni concentrations of 2%, 4%, and 7% to be intrinsic and for 11% Ni concentration to be extrinsic in nature due to precipitation of Ni, and the origin of FM has been attributed to defects mediated.[26] Satyarthi *et al.* have also reported the

*Project supported by the UGC-DAE, Consortium for Scientific Research, Indore through its CRS project bearing No. CSR-IC/MSRSR-12/CRS-220/2017-18/1301.
†Corresponding author. E-mail: skphysics@yahoo.co.in
© 2020 Chinese Physical Society and IOP Publishing Ltd

co-existence of intrinsic and extrinsic origins of RTFM in Ni-ion implanted ZnO films.[27] It has been already reported for Ni-doped ZnO that the nature of FM does not remain intrinsic upon annealing in various environments at high temperature and it may be due to the segregation of TM ions.[28] The FM in hydrogenated and vacuum annealed Ni-doped ZnO has been found to be disappearing upon long reheating in air at very high temperatures of 700 ℃ and 800 ℃, respectively.[29]

The stability and reproducibility in various environments and the attainment of high temperature FM are the most challenging issues in these DMS systems. The nature of FM interaction is little explored in Ni-doped ZnO systems as compared to the Co-doped ZnO systems in experiments. Synthesis of Ni-doped ZnO nanostructures possessing FM above room temperature, appreciable magnetic moment and high crystallinity still remains a significant challenge to be addressed for future spintronic devices. Clearly the magnetism in Ni-doped ZnO is still a subject of much interest that demands careful investigations.

Plenty of researches have been published on ZnO and TM doped ZnO materials. However, a number of issues are still unresolved pertaining to the understanding of the origin of room-temperature global ferromagnetism and band gap changes due to doping. Consequently, arguments and counter arguments have been proposed in subsequent researches.[30] The motivation and the purpose of our present work is to try to develop a further insight and understanding of the complex interesting processes involved in such systems resulting into the evolution of novel functional properties, which can be tuned desirably. The further motivation of our work is to discover an easy, fast and economic low temperature synthesis process for synthesizing such TM doped ZnO materials exhibiting RTFM and possessing useful optical properties in bulk amount in comparatively smaller time.

In the present work, we have synthesized a 10% Ni-doped ZnO system by the wet method of electrodeposition performed at room temperature in open ambience. Our sample exhibits RTFM and also possess interesting optical properties. Different processing procedures have been tried for synthesizing such materials and it is a well-established fact that process parameters of material synthesis sensitively control the structural evolution resulting into newer and novel properties. We know that the same system synthesized through different processes exhibits entirely different structural, magnetic and optical properties. To the best of our knowledge and ample literature survey, synthesis of Ni-doped ZnO DMS with T_c above room temperature by the simple process of electrodeposition has not yet been reported and in that sense our Ni-doped ZnO sample synthesized by single-bath two-electrode electrodeposition exhibiting RTFM is first of its kind to be reported and carries convincing novelty.

2. Material synthesis and experimental details

$Zn_{0.90}Ni_{0.10}O$ has been synthesized by two-electrode electrodeposition in an electrolytic bath. A rectangular gold plate (4 cm × 2.5 cm) was used as the anode and a pure aluminium substrate of the same size as the cathode. The separation between the electrodes was maintained at about 1 mm. We took 50 g of $ZnSO_4{\cdot}7H_2O$ and 8.4 g of $Ni(NO_3)_2{\cdot}6H_2O$ (MERCK purity > 99.9%) dissolved in 200ml of deionized water at room temperature to give the electrolytic bath. Electrodeposition was performed at constant voltage of 5 V for 5 min after which the aluminium substrate was removed from the bath, gently washed with water and then allowed to dry. The applied voltage was supposed to be greater than the reduction potential of the substance deposited at the cathode. The material deposited on the cathode was then gently scrapped and was allowed to oxidize naturally in open atmosphere. This dried sample was then annealed in air at 700 ℃ for 1 hour. This annealed powder has been used in all characterization experiments.

This sample has been characterized using x-ray diffraction (Bruke AXE D8 x-ray diffractometer with Cu K_α radiation $\lambda = 1.54178$ Å) to confirm the crystallographic structure and phase identification. Room-temperature magnetization measurement was carried out using a vibrating sample magnetometer (Lake Shore Cryotronics, Inc., USA) up to an applied field of 2 T. Photoluminescence (PL) and UV-vis-NIR spectroscopy (PerkinElmer, UK) have been obtained to check the doping related changes in band edge emission and absorption spectra, the kind of defects present and their changes due to doping.

3. Results and discussion

The crystal structure of the 10% Ni-doped ZnO sample synthesized by two-electrode single-bath electrodeposition process and subsequently annealed in air at 700 ℃ for one hour has been confirmed by x-ray diffraction using the x-ray diffractometer with Cu K_α radiation ($\lambda = 1.54178$ Å). The XRD pattern is shown in Fig 1(a). In Fig. 1(b), the XRD pattern of undoped ZnO synthesized by the same method under identical conditions and annealed at the same temperature has been shown.

The peak positions of Ni-doped ZnO can very well be attributed to the standard Bragg position of hexagonal wurtzite ZnO. The XRD pattern has been plotted in log scale for the easy confirmation of secondary/impurity phases. It can be seen that no peak corresponding to secondary phases have been observed within the detection limit of x-ray diffractometer, implying thereby that neither Ni segregation has taken place nor other compounds containing Ni, Zn and O_2 have been formed. The XRD pattern show the peaks (100), (002), (101), (102), (110), (103), (112), and (201) of pure hexagonal wurtzite ZnO

phase, which are in good agreement with the JCPDS data. It is also seen that the intensities of different diffraction peaks are different, which signifies that the growth of the crystal structure of ZnO under given conditions in various planes is different and not uniform, thus the growth is polycrystalline and anisotropic. It is also interesting to note that in Ni-doped ZnO the intensity of peaks has been reduced and the FWHM has increased as compared to these values in undoped ZnO prepared by electrodeposition at constant voltage of 5 V and annealed at 700 ℃ for one hour in the presence of air, as shown in Fig 1(b). This is indicative of the fact that the crystalline quality has been degraded due to Ni doping in ZnO and substitution of Zn^{2+} by Ni^{2+}.

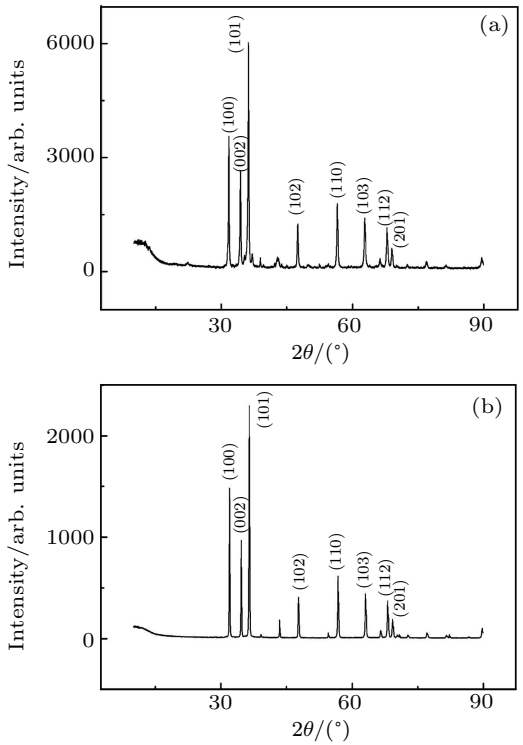


Fig. 1. XRD pattern of (a) Ni-doped ZnO and (b) undoped ZnO, both synthesized by electrodeposition and annealed at 700 ℃ in air for one hour.

It is also worth noting here that the dominant peaks for different planes (100), (002), (101), (102), (110), (103), (112), and (201) have been shifted towards smaller angle direction as compared to the positions of the respective peaks of undoped pure ZnO prepared by the same method under the same conditions and annealed at the same temperature for the same time under identical conditions. The shifting of XRD peaks due to Ni doping in ZnO host towards smaller angle side and absence of any additional impurity phase confirms the evolution of a single-phase hexagonal wurtzite polycrystalline anisotropic ZnO crystal structure with substitution of Zn^{2+} by Ni^{2+} in the lattice. The crystallite size has been calculated by the Scherrer formula

$$D = \frac{K\lambda}{\beta\cos\theta},$$

where K is a constant taken to be equal to 0.89, λ is the wavelength of used x-ray which is 1.54178 Å (Cu $K\alpha$ line), β is the FWHM of the most prominent peak of XRD pattern, 2θ is Bragg's angle.

The lattice parameters have been determined using standard formula for hcp structures taking help of 2θ positions corresponding to different peaks of the XRD pattern

$$\frac{1}{d} = \frac{4}{3}\left[\frac{h^2+hk+k^2}{a^2}\right] + \frac{l^2}{c^2},$$
$$2d\sin\theta = \lambda. \quad (1)$$

The FWHM has been found to be equal to 0.225° and crystallite size to be equal to 41.33 nm. The interplanar spacing corresponding to the most prominent peak is $d = 2.48$ Å.

The lattice parameters have been calculated to be equal to $a = 3.2495$ Å and $c = 5.2069$ Å.

It can be learnt that Ni doping reduces crystallite size as compared to the crystallite size of undoped ZnO grown under identical condition which is equal to 50.84 nm. The reduction in crystallite size due to Ni doping may be thought of as a consequence of the microstructure stress introduced in the crystal due to substitution of Zn^{2+} by Ni^{2+}, which affects the normal growth of ZnO, and the Zener pinning effect may have played a role. It can be seen that the lattice parameters ($a = 3.2495$ Å, $c = 5.2069$ Å) have increased in Ni-doped ZnO as compared to the corresponding values in undoped pure ZnO crystal grown under the identical condition, which are $a = 3.2342$ Å and $c = 5.1772$ Å. This increase in lattice parameters indicates that the volume of Ni-doped ZnO expands slightly. This phenomenon seems difficult to be explained by conventional theories because the ionic radius of Ni^{2+} (0.69 Å) is smaller than the ionic radius of Zn^{2+} (0.74 Å). We believe that there is no new compound formed after doping Ni^{2+} ion but the substitution of Zn^{2+} by Ni^{2+} causes lattice distortion and a large strain has thus been produced in crystal lattice.

As the ionic radius of Ni^{2+} is smaller than the ionic radius of Zn^{2+} the residual stress generated during the crystallization process causes an increased mutual repulsion between the Ni^{2+} ion polarization charges. The system energy thus rises, which triggers the volume increase. The increase in volume may also be assumed to cause a change in oxygen parameter.

In consideration of the above-mentioned facts on the basis of the analysis of x-ray diffraction pattern of Ni-doped ZnO, it can be discerned that a good quality hexagonal wurtzite polycrystalline ZnO crystal structure has evolved by the electrodeposition method.

The optical behavior and properties of our sample have been studied using UV visible spectroscopy and photoluminescence (PL) spectroscopy. The UV visible and PL spectroscopies are used for studying energy band gap value and modification in the energy band structure due to doping and also to study the absorption and emission properties of the material.

A distinct shift in blue region can be observed in the absorption edge for the Ni-doped ZnO nano-particles as compared to undoped ZnO nano-particles. The observed blue shift is indicative of a modification in the band structure due to incorporation of Ni ions in Ni-doped nano-structures. The dopants are supposed to break the periodicity of the lattice and hence they perturb the band structure locally. A new energy level in the band gap is likely to be created due to Ni doping in ZnO lattice.

Since Ni exists in Ni^{2+} oxidation state, there is an appreciable difference in the electronic configuration of Zn^{2+} and Ni^{2+}.

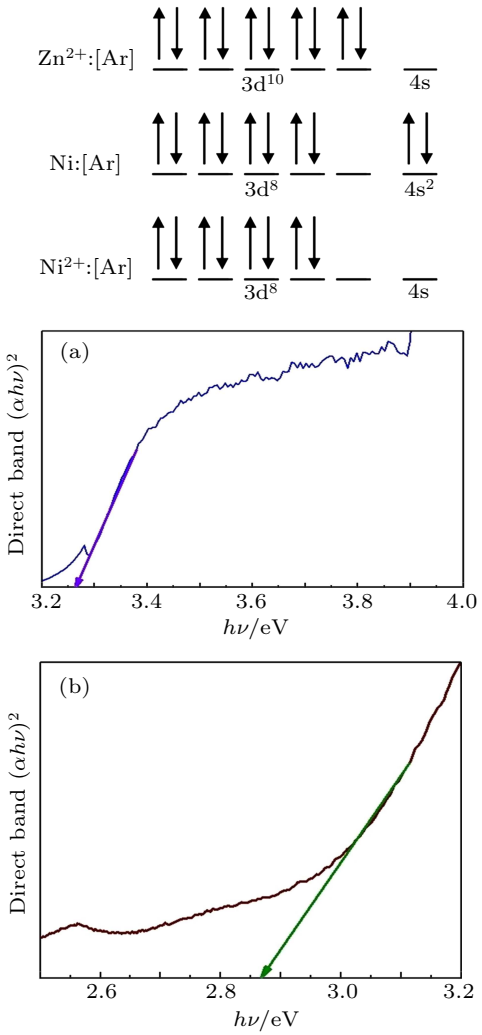


Fig. 2. (a) UV visible graph of un-doped ZnO (synthesized by electrodeposition and annealed at 700 °C in air for one hour) for absorbance and band gap determination. (b) UV visible graph of Ni-doped ZnO (synthesized by electrodeposition and annealed at 700 °C in air for one hour) for absorbance and band gap determination.

Two electrons missing from the orbital of Ni^{2+} as compared to Zn^{2+} ions which have all the orbitals of their d-subshell full cause shifting of the lowest occupied molecular orbital (LUMO) of conduction band as well as the highest occupied molecular orbital (HOMO) of valence band in doped ZnO as compared to the LUMO and HOMO in pure ZnO. The LUMO of the conduction band of the $Zn_{0.90}Ni_{0.10}O$ is expected to have shifted downwards as compared to the LUMO of pure ZNA samples. The HOMO of valence band of $Zn_{0.90}Ni_{0.10}O$ also shifts downwards as compared to the HOMO of the pure ZnO sample, while the downward shifting of the LUMO of conduction band of $Zn_{0.90}Ni_{0.10}O$ is greater in comparison to the downward shifting of the HOMO of valence band of $Zn_{0.90}Ni_{0.10}O$, also compared to the corresponding values in pure ZnO. Thus, the narrowing of the band gap in the doped ZnO may mainly be attributed to the downward shift of the conduction band.

Hence, the exchange interaction between the Sp-d ZnO band electrons and localized d-electrons of the doped Ni^{2+} ions may be considered to be a cause of the change in band structure.[31,32] The UV-visible spectroscopy analysis as shown in Fig. 2(b) exhibits that the optical band gap has decreased due to Ni-doping in ZnO. In Ni-doped ZnO the energy band gap has been found to be equal to 2.87 eV as shown in Fig. 2(b), which is 3.26 eV in the case of pure ZnO synthesized under identical condition as shown in Fig. 2(a). The decrease in optical energy gap substantiates the fact that Ni^{2+} has beautifully substituted Zn^{2+} and a single-phase hcp wurtzite structure has evolved.

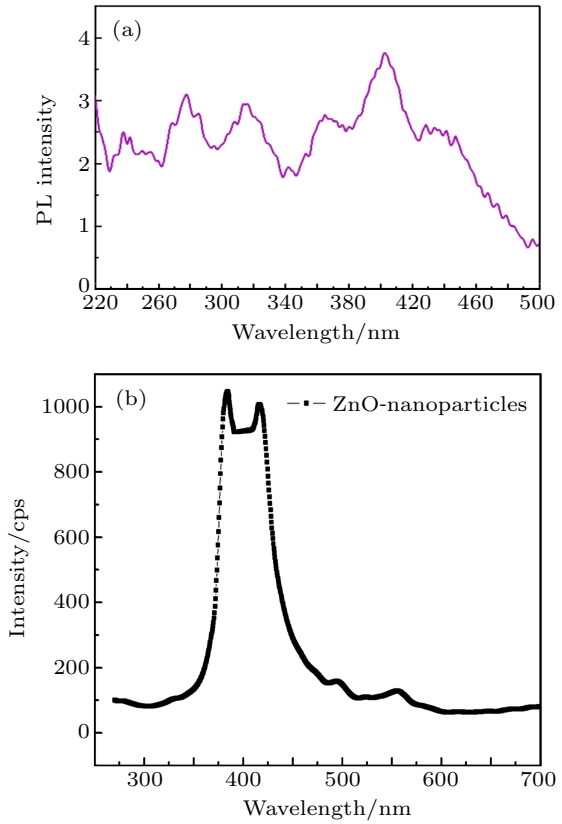


Fig. 3. (a) PL spectra of Ni-doped ZnO synthesized by electrodeposition and annealed at 700 °C in air for one hour. (b) PL spectra of undoped ZnO synthesized by electrodeposition and annealed at 700 °C in air for one hour.

PL spectroscopy is used as an effective tool for investigating the presence of defects which usually play a crucial role in inducing FM ordering in ZnO based DMS. The room-

temperature PL studies for the Ni-doped and pure ZnO nanoparticles reveal UV emission peaks and a broad visible emission band ranging from 380 to 420 nm as shown in Figs. 3(a) and 3(b), respectively.

The presence of these PL peaks in the visible region is indicative of the existence of multicomponent. Undoped ZnO nano-particles exhibit an emission peak at 380 nm (3.26 eV). Ni-doped ZnO NPs show a shift in blue region in this NBE emission peak. This blue shift can be attributed to the strong exchange interaction between the d electrons of Ni ions and the S-p electron of the host band.

A blue emission peak centered at 410 nm (3.03 eV) may be attributed to the presence of Zn_i related surface defects. As the emission originating due to O_i in the red and near IR regions is not observed in the PL emission spectrum of our sample and the blue emission corresponding to Zn_i is observed, we expect that our sample is Zn rich. Hence Zn_i and O_v defects are expected to be responsible for the visible emission. Some less prominent emission peaks centered at 425 nm and 445 nm and between 460 nm and 500 nm may be attributed to oxygen vacancies.

The formation of a new dopant level between the valence band and the conduction band may have enhanced the photocatalytic activity of the Ni-doped ZnO nano structure. It is also found that the sample shows good optical transmittance in near UV and visible region and hence our sample is a potential candidate to be used as a UV sensor. The sample is Zn rich and a large number of oxygen vacancies exist, which may be supposed to play an important role in inducing FM ordering in the sample.

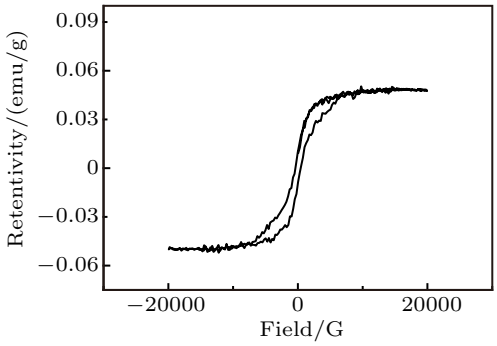


Fig. 4. VSM graph of Ni-doped ZnO synthesized by electrodeposition and annealed at 700 ℃ in air for one hour.

To know the magnetic property of our 10% Ni-doped ZnO crystal grown by the wet method of electrodeposition at ambient temperature and constant voltage of 5 V and then annealed at 700 ℃ for one hour in air for crystallization to take place magnetization versus magnetic hysteresis plot was recorded at room temperature using vibrating sample magnetometer whose field versus magnetization curve is shown in Fig. 4.

The magnetization versus the applied magnetic field curve reveals a magnetic hysteresis behavior.

The coercivity of the sample has been found to be equal to 263 G and the retentivity has been found to be equal to 6.16×10^{-3} emu/g. The room-temperature saturation magnetization has been found to be equal to 50×10^{-3} emu/g.

The clear magnetization versus magnetic field hysteresis loop is indicative of a magnetically ordered state at room temperature. The origin of this room-temperature weak ferromagnetism exhibited by ZnO based dilute magnetic semiconductors has been tried to be explained on the basis of diverse theories. The magnetic property of such systems may depend on a number of parameters such as the distribution and concentration of the TM ions, morphology of the host lattice, type and concentration of defects. Due to high surface-to-volume ratio in ZnO nanoparticles (NPs), the surface effects are very pronounced. There are two interacting subsystems in such DMS materials: (1) the diluted system of localized magnetic moments associated with the TM ions and (2) the delocalized conduction band electrons and valence band holes. The coupling of the spins of s-like electrons or p-like holes near the band edges to the d-shell spins of the TM ions may cause ferromagnetic interaction.

The Zener model has been proposed for the exchange interactions between the carriers and localized spins (s–d interaction). Later, Dietl *et al.* took help of Zener description and realized that the origin of RTFM may be due to hole mediated exchange interactions and they could theoretically predict a curie temperature above room temperature in p-type ZnO with 5% Mn dopants and a carrier concentration of 3.5×10^{20} holes/cm^3.

An important role is being played by the intrinsic defects (zinc vacancies V_{Zn}, interstitial oxygen O_i, oxygen vacancy V_O, zinc interstitial Zn_i, etc.) in inducing the FM interaction in TM doped ZnO based DMS systems. The requirement of a long-range interaction necessary to obtain high temperature FM ordering in TM doped DMS systems was supposed to be mediated by defect induced states.

The bound magnetic polaron (BMP) model proposes that the bound electrons (holes) in the defect states are supposed to couple with TM ions and cause the ferromagnetic regions to overlap, which gives rise to long-range FM ordering. The sp–d interaction often leads to the formation of BMPs. The proposition of the BMP model assumes that in the presence of donors or acceptors the bound electrons (holes) together with the spins of the TM ions are within a hydrogenic Bohr orbit of radius R_h (for ZnO, $R_h = 0.76$ nm). Due to the sp–d interaction a significant net ferromagnetic alignment is obtained in the spins of transition metal ions.

Very recently, ZnO based dilute magnetic semiconducting systems doped with group V elements have been found to exhibit d^0 magnetism and has attracted a great deal of attention from researchers.[33] For example, C-doped ZnO has been extensively studied theoretically as well as experimen-

tally, and has been found to exhibit room-temperature d^0 ferromagnetism.[34–36]

A ZnO host doped with a group V element will usually exhibit spin polarized RTFM if either an oxygen is substituted by the dopant (X_O) or a Zn is substituted by group V dopant with two Zn vacancies (X_{Zn}–$2V_{Zn}$). The formation of a magnetic moment requires a strong localization of orbitals. The 3d and 2p orbitals show relatively strong localization and therefore 2p light element doped ZnO is supposed to be more likely to show d^0 ferromagnetism. Furthermore, the study of Lu *et al.*[33] confirmed that not only the 2p elements but the 3p, 4p and 5p dopants could also make ZnO a dilute magnetic semiconducting system.

Among these X related defects only X_O and X_{Zn}–$2V_{Zn}$ complexes have been found to be magnetic while X_{Zn} complexes are usually non-magnetic. It is proposed that holes are more effective than electrons in contributing magnetic moments in such semiconductors. X_{Zn} defects acts as donors and provide additional electrons as free carriers that are no longer localized around the impurity. The spins of these free electrons are randomly spread all over the crystal lattice and hence their spins average out to zero and therefore the materials containing X_{Zn} defects do not show macroscopic magnetism.

N-doped ZnO has been found to exhibit RTFM. The ferromagnetic coupling in N-doped ZnO is likely to be resulting from the partially filled N-2p states and O-2p and Zn-3d states surrounding the defect. N-2p states overlap significantly with those of O-2p and Zn-3d states near the Fermi energy, suggesting that a strong coupling interaction among them results in the splitting of the energy levels near Fermi energy. The coupling of Zn-3d and N-2p between the N ion and the nearest neighbors surrounding Zn ions is described as p–d coupling.[37] The N-2p orbital could also couple with the next nearest neighbors O-2p orbitals due to its delocalized nature, which results from the overlap between p states and the host p states at the top of the valence band and this is named as p–p coupling.[38]

In our sample we expect the Ni atoms to be in tetrahedral crystal field. The 5-fold degeneracy of the Ni 3d band has been transformed to a 3-fold degenerate t_{2g} state and a 2-fold degenerate e_g states. We propose that in accordance with Hund's rule and double exchange mechanism an FM coupling is expected to have taken place. The replacement of Zn^{2+} ions with Ni^{2+} ions causes the formation of an occupied t_{2g} orbital.

This is a ferromagnetic (FM) state with lowest possible energy since six electrons occupy t_{2g} orbitals and two electrons occupy e_g orbitals. As a result, the spin of electrons of Ni^{2+} e_g states and the neighboring Ni^{2+} e_g states are aligned in the same direction, and hence Ni^{2+} ions are able to couple to each other and move between the two neighboring Ni^{2+} ions, resulting in a stable FM coupling in such Ni-doped ZnO systems.

Our sample has been synthesized by the method of electrodeposition at ambient temperature and constant voltage, then annealed at 700 ℃ for one hour for crystallization to take place, and so the sample is expected to be containing a lot of defects such as oxygen vacancy (O_v) and zinc interstitial (Zn_i) because the process of electrodeposition is known for creating a lot of defects. Annealing at high temperature and substitution of Zn^{2+} ions by Ni^{2+} ions in pure phase of ZnO hcp wurtzite crystal structure are likely to have induced strain in crystal, and thus contribute to several crystal imperfections.

We know that the interaction of intrinsic carriers with the oxygen vacancies plays a significant role in BMP formation because the electrons locally trapped by oxygen vacancies may couple with Ni^{2+} ions and cause FM regions to overlap, which gives rise to a long-range FM ordering. In this defect mediated RTFM, the large density of oxygen vacancy helps to provide more BMPS and enhance FM ordering.

Hence, we may conclude that basically the double exchange mechanism and the defect induced BMP model is responsible to induce room-temperature global FM ordering in our sample.

4. Conclusion

A single-phase polycrystalline hcp wurtzite crystal structure of pure ZnO has been confirmed by x-ray diffraction pattern peak positions. Microstructure stress has been found to exist in the crystal, which has resulted the volume of Ni-doped ZnO to expand slightly. This strain produced in the crystal due to Ni doping has resulted in the lattice parameters to increase slightly despite the fact that the ionic radius of Ni^{2+} is smaller than ionic radius of Zn^{2+}. The nickel atoms are likely to be in tetrahedral crystal field and a ferromagnetic coupling is expected to have taken place by double exchange mechanism to induce room-temperature ferromagnetic ordering in the system. The sample is likely to be Zn rich and contain a large number of oxygen vacancies, which has facilitated the condition for bound magnetic polaron to be formed, and thus defect induced RTFM is also expected to have played a role for the sample to exhibit magnetic hysteresis behavior at room temperature. UV vis and PL studies confirm the substitution of Zn^{2+} by Ni^{2+} and the presence of crystal defects such as zinc interstitial (Zn_i) and oxygen vacancies (O_v). The synthesized sample seems to be a potential candidate used as UV sensors.

Acknowledgment

One of the authors, Santosh Kumar, acknowledges Mr. Kshitij Kashyap for a productive discussion on Crystal Field Theory. We deeply acknowledge Mr. Kumar Ashay for his invaluable technical support.

References

[1] Wolf S A, Awschalom D D, Nuhrman R A, Daughton J M, Molnar S V, Roukes M L, Chtchelkanova A Y and Tregger D M 2001 *Science* **294** 1488

[2] Sarma S D 2001 *Am. Sci.* **89** 516

[3] Zntic I, Fabian J and Sarma S D 2004 *Rev. Mod. Phys.* **76** 323

[4] Awschalom D D and Flatte M E 2007 *Nat Phys.* **3** 153

[5] Felser C, Fecher G H and Balke B 2007 *Angew Chem.* **46** 668

[6] Furdyna J K 1988 *J. Appl. Phys.* **64** R29

[7] Ohno H 1998 *Science* **281** 951

[8] Dietl T, Ohno H, Matsukura F, Cibbert J and Ferrand D 2000 *Science* **287** 1019

[9] Dietl T 2002 *Semicond. Sci. Technol.* **17** 377

[10] Dietl T 2003 *Nat. Mater.* **2** 646

[11] Prellier W, Fouchet A and Mercey B 2003 *J. Phys.: Condens. Matter* **15** R1583

[12] Pearton S J, Heo W H, Ivill M, Norton D P and Steinner T 2004 *Semicond. Sci. Technol.* **19** R59

[13] Bryan J D and Gainelin D R 2005 *Prog. Inorg. Chem.* **54** 47

[14] Macdonald A H, Schiffer P and Samarth N 2005 *Nat. Mater.* **4** 195

[15] Kuroda S, Nishizawa N, Takita K, Mitome M, Bando Y, Osuch K and Dietl T 2007 *Nat. Mater.* **6** 440

[16] Sundaresan A and Rao C N R 2009 *Nano Today* **4** 96

[17] Pan F, Song C, Liu X J, Yang Y C and Zeng F 2008 *Mater. Sci. Eng. R* **62** 1

[18] Potzat K and Zhou S 2009 *Phys. Status Solid B* **246** 1147

[19] Janisch R, Gopal P and Spladin N A 2005 *J. Phys.: Conden Matter* **17** R657

[20] Ogale Satishchandra B 2010 *Adv. Mater.* **22** 3125

[21] Wakano T, Fujimura N, Morinaga Y, Abe N and Ashida A 2001 *Physica E* **10** 260

[22] Schwartz D A, Kittils K R and Gamellin D R 2004 *Appl. Phys. Lett.* **85** 1395

[23] Radovanovic P V, Norberg N S, Menally K E and Gamellin D R 2002 *J. Am. Chem. Soc.* **124** 15192

[24] Srinet G, Kumar R and Sajal V 2013 *J. Appl. Phys.* **114** 033912

[25] Liu X, Lin F, Sun L, Cheng W, Ma X and Shi W 2006 *Appl. Phys. Lett.* **88** 062508

[26] Liu X J, Zhu X Y, Song C, Zeng F and Pan F 2009 *J. Phys. D: Appl. Phys.* **42** 035004

[27] Satyarthi P, Ghosh S, Pandey B, Kumar P, Chen C L, Dong C L, Pong W F, Kanjibal D, Asokan K and Srivastava P 2013 *J. Appl. Phys.* **113 18** 183708

[28] Tong L N, He X M, Han H B, Hu J L, Xia A L and Tong Y 2010 *Solid State Commun.* **150** 1112

[29] Singhal R K, Sharma S C, Kumari P, Kumar S, Xig Y T, Deshpande U P, Shripak T and Saitovitch E 2011 *J. Appl. Phys.* **109** 063907

[30] Samanta Anindita, Goswami, M N and Mahapatra P K 2018 *J. Alloys Compd.* **730** 399

[31] Ali M, Sharif S, Anjum S, Imran M, Ikram M, Naz M and Ali S 2020 *Mater Res. Express* **6** 1250d5

[32] Mishra Prashant Kumar, Amin Rahul, Biring Sajal and Sen Somaditya 2019 *AIP Conf. Proc.* **2100** 020121

[33] Lu Y B, Dai Y, Guo M, Yu L and Huang B B 2013 *Phys. Chem. Chem. Phys.* **15** 5208

[34] Yang K S, Wu R Q, Shen L, Feng Y P Dai Y and Huang B B 2010 *Phys. Rev.* **81** 125211

[35] Pan H, Yi J B, Shen L, Wu R Q, Yang J H, Lin J Y, Feng Y P, Ding J, Van L H and Yin J H 2007 *Phys. Rev. Lett.* **99** 127201

[36] Nayak Sanjeev K, Gruner E, Sakong Sung, Sil Shreekantha, Kartzer Peter, Behera N and Entel Peter 2012 *Phys. Rev. B* **86** 054441

[37] Liu L, Peter Y, Yu, Ma Z X and Mao S 2008 *Phys. Rev. Lett.* **100** 127203

[38] Shen L, Wu R Q, Pan H, Peng G W, Yang M, Sha Z D and Feng Y P 2008 *Phys. Rev. B* **78** 073306